ADVANCED CONTROL FOR PHOTOVOLTAIC-UNIFIED POWER QUALITY CONDITIONER SYSTEMS: A SIMULATION APPROACH

LAKHDAR SAIHI1*, BRAHIM BERBAOUI2

Keywords: Unified power quality conditioner (UPQC); P-Q theory; Photovoltaic (PV) system; Sliding mode control (SMC); Adaptive neuro-fuzzy inference (ANFIS) systems.

This paper presents the design and evaluation of a three-phase photovoltaic-unified power quality conditioner (PV-UPQC), integrating series and shunt compensators via a shared DC link. The system combines distributed generation with active power filtering, where the shunt compensator harvests PV power and compensates for harmonic currents and reactive power from nonlinear loads. Harmonic identification uses p-q theory, with experiments conducted under real solar irradiation in Algeria's Adrar region. The shunt active power filter (ShAPF) compensates for harmonics and reactive power while optimizing PV power extraction at the maximum power point (MPP). Adaptive neuro-fuzzy inference systems (ANFIS) and sliding mode control (SMC) are combined to reduce chattering and enhance PV energy extraction. Simulations show SMC/ANFIS outperforms conventional SMC.

1. INTRODUCTION

The integration of renewable energy systems like solar PV and wind energy into modern distribution systems is driven by environmental concerns but poses challenges due to their intermittent nature [1, 2]. Power electronics-based loads, which are highly nonlinear, exacerbate these issues, leading to power quality problems such as voltage sags, swells, interruptions, flicker, and grid instability. These issues can cause malfunctions in electronic systems and increased heating of capacitor banks [1]. Nonlinear loads inject harmonics into the distribution system, distorting the point of common coupling (PCC) voltage, particularly in weak grids, and resulting in losses in distribution cables and transformers [3].

To tackle power quality challenges in distribution systems, custom power devices such as DSTATCOM, DVR, and UPQC are used [4]. DSTATCOM, a shunt-connected system, addresses issues like reactive current, harmonics, and load imbalance. DVR, a series-connected system, resolves grid voltage sag and swell problems [5]. UPQC, integrating both shunt and series compensators, combines the functionalities of DSTATCOM and DVR, providing comprehensive power quality improvement [1].

In recent developments in control systems, various advanced nonlinear techniques have emerged to effectively manage PV solar systems integrated with UPQC to mitigate harmonic currents and reactive power. Sliding mode control (SM-C), as discussed in [6, 7-10], stands out as a sophisticated methodology tailored for controlling nonlinear systems. Its primary goal is to guide the controlled dynamics of the system toward a designated sliding surface, maintaining it until equilibrium is achieved. Several research studies have demonstrated the practical application and effectiveness of SM-C. In [6], two distinct strategies were presented: the conventional PI controller and the SM-C of a three-phase ShAPF, with a subsequent comparison of these approaches. Additionally, in [7], a comparative study involving simulation and experimentation was introduced, evaluating the SM-C against a PI regulator in the context of controlling the DC bus voltage of a three-phase ShAPF.

In [8], a vector operation technique for governing threephase converters using one-cycle control was introduced, incorporating a comprehensive large-signal model for a threephase APF. The study developed SM-C within innovative coordinates, coupled with a modulator for generating control signals in the natural frame. In [9], an adaptive dynamic special global SM-C for a three-phase APF was proposed, utilizing a PID sliding surface and integrating an RBF neural network to enhance robustness and minimize chattering effects. [10] introduced continuous terminal sliding mode control using a meta-cognitive fuzzy neural network for an APF, aiming to minimize tracking errors within a finite time. However, SM-C's ripple effects, resulting from discontinuous control switching functions, can degrade power quality and introduce additional harmonics. Therefore, alternative robust strategies are being explored to address this challenge and enhance classical SM-C performance.

This research proposes employing hybrid control methods to mitigate ripple effects in power systems, replacing traditional approaches with artificial intelligence techniques like fuzzy logic control (FLC) or artificial neural networks (ANN). However, conventional FLC systems may require expert knowledge for rule definition and parameter tuning, while ANN approaches might lack adequacy in covering all operational states with limited training data. To address these challenges, the study introduces the adaptive neuro-fuzzy inference system (ANFIS), combining the learning capabilities of ANNs with the inference abilities of fuzzy logic. This hybrid ANFIS approach offers a comprehensive solution, overcoming the limitations of individual techniques. Implemented as SMC/ANFIS in a three-phase ShAPF, it effectively mitigates ripple effects and enhances power quality, presenting a more advanced and intelligent control approach through the integration of artificial neural networks.

2. CONFIGURATION OF PV-UPQC SYSTEM

The Photovoltaic-Unified Power Quality Conditioner (PV-UPQC) integrates a photovoltaic (PV) system into a three-phase configuration through a shared DC link [1, 2]. The system comprises a shunt active power Filter (ShAPF) connected in parallel to the AC grid on the load side and a Series Active power filter (SeAPF) connected in series with the grid. The PV array is directly integrated via a reverse blocking diode, while interfacing inductors connect both compensators to the grid. Ripple filters are employed to mitigate harmonics generated by converter switching. As a custom power device, the UPQC enhances power quality by addressing issues such as harmonics, reactive power, voltage regulation, imbalance, sag/swell, and interruptions [1, 3].

¹ Unité de Recherche en Énergies Renouvelables en Milieu Saharien URERMS, Centre de Développement des Énergies Renouvelables CDER, 01000 Adrar, Alegria. (corresponding author)

² Department of Electrical and Computer Engineering, University of Draia Ahemed Adrar, 01000 Adrar, Algeria. E-mails: saihi_lakhdar@urerms.dz, berbaoui.brahim@univ-adrar.edu.dz

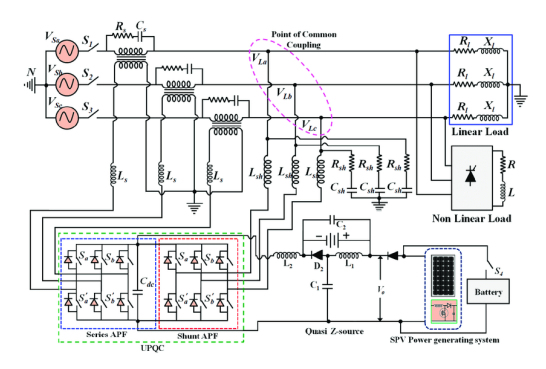


Fig. 1 – PV-UPQC system configuration.

The study focuses on controlling the ShAPF, depicted in Fig. 1 [6, 8]. The power circuit features a conventional two-level six IGBTs PWM inverter, connected to the AC grid via a first-order L-type passive filter with parameters L_f and R_f [11–13]. A DC-bus capacitor (C_{dc}) on the DC side maintains the voltage v_{dc} . According to Kirchhoff's current law, the active filter current is $i_{fabc} = i_{sabc} - i_{labc}$. This means the active filter must absorb harmonics from the nonlinear load in the opposite phase to ensure a sinusoidal source current in abc coordinates [14, 15]. Additionally, the active filter is designed to enhance the power factor on the grid side [16, 17].

The power grid consists of three voltages that create a balanced three-phase system, which can be represented as follows [1, 6, 7]:

$$\begin{bmatrix} v_{sa} \\ v_{sb} \\ v_{sc} \end{bmatrix} = v_{sm} \begin{bmatrix} \sin(\omega_n t) \\ \sin(\omega_n t - \frac{2\pi}{3}) \\ \sin(\omega_n t - \frac{4\pi}{3}) \end{bmatrix}. \tag{1}$$

where; v_{sm} : the voltage source, ω_n : the frequency of the system.

The interaction between the ShAPF and the grid is elucidated through the average dynamic model in d-q coordinates, as provided below [2, 3, 8]:

$$\begin{bmatrix} i_{fd} \\ i_{fq} \end{bmatrix} = A \begin{bmatrix} i_{fd} \\ i_{fq} \end{bmatrix} + B \left(\begin{bmatrix} v_{fd} - v_{ld} \\ v_{fq} - v_{lq} \end{bmatrix} \right) = X. \tag{2}$$

where; $\begin{bmatrix} \frac{-R_r}{L_f} & \omega_s \\ -\omega_s & \frac{-R_r}{L_f} \end{bmatrix} = A$, $\begin{bmatrix} \frac{1}{L_f} & 0 \\ 0 & \frac{1}{L_f} \end{bmatrix} = B$.

The voltage on the DC side of the ShAPF:

$$[\dot{v}_{dc}] = \left[\frac{1}{c_{dc}}\right] [i_{dc}]. \tag{3}$$

3. PV-UPQC CONTROL STRATEGY

3.1. HARMONICS IDENTIFICATION

Accurate extraction and estimation of harmonics are essential for assessing the ShAPF's effectiveness. Various methods are utilized to compute the reference current, classified into time domain analysis and frequency domain analysis. Time domain analysis offers simplicity with fewer calculations, while frequency domain analysis is more complex and resource intensive. This study introduces P-Q theory (active and reactive power) in the time domain, employing MATLAB/Simulink to develop a simulation model. The theory involves transforming stationary reference coordinates into rotating coordinates using Clarke transformation, effectively eliminating the DC component

from power calculations. This process is illustrated in Fig. 2, depicting the P-Q harmonic current extraction theory [18, 19].

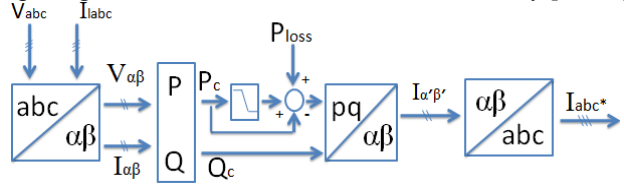


Fig. 2 - "P-Q" theory.

3.2 SLIDING MODE CONTROL FOR SHUNT ACTIVE POWER FILTER (SHAPF)

Sliding Mode Control (SM-C) is a robust nonlinear control technique recognized for its ability to regulate complex systems effectively, even in the presence of varying parameters. It guides the trajectory dynamics of the controlled system to adhere to a predefined sliding surface until achieving equilibrium. Despite its effectiveness, SM-C can introduce undesirable fluctuations, known as chattering, which may impact power grid quality. Recent efforts have aimed to mitigate these challenges, enhancing the appeal of SM-C. Typically, the design process of SM-C involves selecting the sliding surface, identifying system conditions, and formulating control laws, often guided by conditions defined by the Lyapunov function [20, 21].

$$S\dot{S} < 0. \tag{4}$$

The nonlinear expression formulation for the sliding surface (*Slotine*) was derived [20, 21]:

$$s(t) = \left(\lambda_s + \frac{\mathrm{d}}{\mathrm{d}t}\right)^{n-1} e(t). \tag{5}$$

where $\lambda_s > 0$, r(t) and y(t)were, desired and real dynamic, respectively; n: the relative degree, e(t): error of the variable to be adjusted [20, 21]:

$$e(t) = y(t) - r(t). \tag{6}$$

The main goal of ShAPF is to address harmonics and reactive power requirements arising from nonlinear loads. Its controller synthesis involves cascading two loops. Firstly, an inner current loop utilizes two nonlinear regulators to compensate for reactive and harmonic power, enabling the generation of sinusoidal input currents synchronized with grid voltages. Secondly, an outer loop is established to regulate voltage on the DC side of the ShAPF, thereby enhancing overall system performance [6–8].

3.1.1 FORMULATING THE INNER LOOP FOR CURRENT REGULATION

The first step in the design process involves selecting switching surfaces for the current inner loop of the ShAPF. SM functions tailored for tracking the reference electric current are determined. A global sliding surface is then defined, comprising a conventional SM manifold augmented with an integral term to enhance both transient and steady-state performances [6, 7, 8]:

$$S(X) = k_n E(X) + k_i \int e(X) dt.$$
 (7)

The tracking error is:

$$e(X) = (X^* - X).$$
 (8)

Let's present the current tracking errors i_{fd} , i_{fq} [9, 10]:

$$\begin{bmatrix} e(i_{fd}) \\ e(i_{fq}) \end{bmatrix} = \begin{bmatrix} (i_{fd}^* - i_{fd}) \\ (i_{fq}^* - i_{fq}) \end{bmatrix}. \tag{9}$$

If we substitute Eq. (2) with Eq. (8), we get:

$$\begin{bmatrix} e(i_{fd}) \\ e(i_{fq}) \end{bmatrix} = \begin{bmatrix} i_{fd}^* \\ i_{fq}^* \end{bmatrix} - \left(A \begin{bmatrix} i_{fd} \\ i_{fq} \end{bmatrix} + B \left(\begin{bmatrix} v_{fd}^* - v_{ld} \\ v_{fq}^* - v_{ld} \end{bmatrix} \right) \right) = E. \quad (10)$$

The derivation of the sliding surfaces can be inferred from equations (8) and (9) as follows:

$$\begin{bmatrix} S(i_{fd}) \\ S(i_{fq}) \end{bmatrix} = \begin{bmatrix} k_d & k_{id} \\ k_q & k_{iq} \end{bmatrix} \begin{bmatrix} e(i_{fd}) & e(i_{fd}) \\ f(i_{fq}) dt & f(i_{fq}) dt \end{bmatrix}.$$
(11)

In the SM-C, the conditions are specified as follows:

$$\begin{bmatrix} S(i_{fd}) \\ S(i_{fq}) \end{bmatrix} = \begin{bmatrix} 0 \\ 0 \end{bmatrix} \text{ and } \begin{bmatrix} \dot{S}(i_{fd}) \\ \dot{S}(i_{fq}) \end{bmatrix} = \begin{bmatrix} 0 \\ 0 \end{bmatrix}.$$

The derivative of $S(i_{fd})$ and $S(i_{fq})$ with respect to time is expressed by:

$$\begin{bmatrix} \dot{S}(i_{fd}) \\ \dot{S}(i_{fq}) \end{bmatrix} = \begin{bmatrix} k_d & 0 \\ 0 & k_q \end{bmatrix} (E) + \begin{bmatrix} k_{id} & 0 \\ 0 & k_{iq} \end{bmatrix} \begin{bmatrix} e(i_{fd}) \\ e(i_{fq}) \end{bmatrix} = \begin{bmatrix} 0 \\ 0 \end{bmatrix}. (12)$$

The control law "u" can be divided into two parts: the first component being the discontinuous control " u_{dis} ", and the second being the equivalent control " u_{eq} ".

$$u = u_{eq} + u_{dis} = \begin{bmatrix} u_{fd}^{eq} + u_{fd}^{dis} \\ u_{fq}^{eq} + u_{fq}^{dis} \end{bmatrix} = \begin{bmatrix} v_{fd}^* \\ v_{fq}^* \end{bmatrix}.$$
(13)

The equivalent law: From Eq (11), the equivalent control u_{fd}^{eq} and u_{fg}^{eq} can be defined as follows [6, 7, 10]:

$$\begin{bmatrix} u_{fd}^{eq} \\ u_{fq}^{eq} \end{bmatrix} = \left(\begin{bmatrix} k_d B \\ k_q B \end{bmatrix} \right)^{-1} \left[\left(\begin{bmatrix} k_d X \\ k_q X \end{bmatrix} \right) + \left(\begin{bmatrix} k_{id} e(i_{fd}) \\ k_{iq} e(i_{fq}) \end{bmatrix} \right) \right]. \tag{14}$$

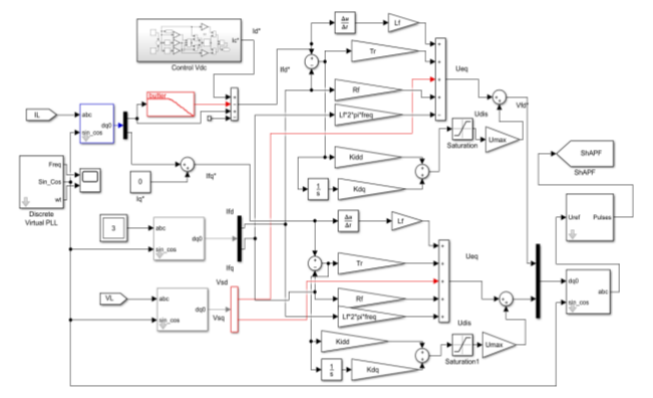


Fig. 3 – The internal loop for current regulation using SM-C.

The discontinuous law: when trajectories deviate from the sliding surface state, discontinuous control is utilized to minimize the gap between the trajectory and the sliding surface, ensuring convergence to the reference. The formulation of the discontinuous control function in real-world scenarios is determined based on methodologies outlined in [8–10]:

$$\begin{cases} u_{fd}^{dis} = \begin{bmatrix} U_{max} & 0 \\ 0 & -U_{max} \end{bmatrix} \begin{bmatrix} sat \ S(i_{fd}) \\ sat \ S(i_{fd}) \end{bmatrix} & \text{if } S(i_{fd}) > 0 \\ sat \ S(i_{fd}) \end{bmatrix} & \text{if } S(i_{fd}) < 0 \\ u_{fq}^{dis} = \begin{bmatrix} U_{max} & 0 \\ 0 & -U_{max} \end{bmatrix} \begin{bmatrix} sat \ S(i_{fq}) \\ sat \ S(i_{fq}) \end{bmatrix} & \text{if } S(i_{fq}) > 0 \end{cases}$$
(15)

The control can be expressed as follows:

$$\begin{bmatrix} v_{fd}^* \\ v_{fq}^* \end{bmatrix} = \begin{bmatrix} u_{fd} \\ u_{fq} \end{bmatrix} = \begin{bmatrix} u_{fd}^{eq} \\ u_{fq}^{eq} \end{bmatrix} + \begin{bmatrix} u_{fd}^{dis} \\ u_{fq}^{dis} \end{bmatrix}. \tag{16}$$

Figure 3 illustrates the internal current control loop employing an SM-C for Shapf:

3.2.1 FORMULATING THE EXTERNAL LOOP FOR DC VOLTAGE REGULATION

The ShAPF's control strategy focuses on maintaining a stable DC voltage on the inverter's DC side by regulating the DC-link voltage for efficient harmonic current compensation. While DC-link capacitors ideally keep the voltage constant with minimal real power exchange, a small amount of real power is needed for the inverter's switching operations [6, 7, 10].

To achieve the target of constant DC-link voltage and effective harmonic current compensation, a sliding mode control (SM-C) is implemented in the DC-link voltage control loop. This entails comparing the DC-link capacitor voltage (v_{dc}) with a reference DC voltage (v_{dc}^*) . The resulting error $(e(v_{dc}) = v_{dc}^* - v_{dc})$ serves as the input to the SM-C. The SM-C plays a pivotal role in eliminating steady-state errors in the reference current signal tracking process. This design ensures robust DC-link voltage regulation, contributing to the overall stability and effectiveness of the ShAPF in compensating harmonic currents. The expression for the sliding surface governing DC voltage control is articulated as follows [10]:

$$[S(v_{dc})] = \begin{bmatrix} k_1 & k_2 & k_3 \end{bmatrix} \begin{bmatrix} e(v_{dc}) \\ \dot{e}(v_{dc}) \\ \int e(v_{dc}) dt \end{bmatrix}. \tag{17}$$

In the sliding mode control (SM-C) framework, the expressions for the switching functions u_1 and u_2 are outlined to regulate the direct current (DC) voltage of the capacitor (v_{dc}) [6, 7, 10].

$$\begin{cases} u_{1} = \begin{bmatrix} u_{1_max} \\ -u_{1_max} \end{bmatrix} & if \ S(e(v_{dc}))e(v_{dc}) > 0 \\ if \ S(e(v_{dc}))e(v_{dc}) < 0 \\ u_{2} = \begin{bmatrix} u_{2_max} \\ -u_{2_max} \end{bmatrix} & if \ S(e(v_{dc}))\dot{e}(v_{dc}) > 0 \\ if \ S(e(v_{dc}))\dot{e}(v_{dc}) < 0 \end{cases}$$
(18)

Therefore, the output of this sliding mode control (SM-C) is defined as:

$$[u_{v_{dc}}] = [i_{dc}] = [k_4 \quad k_5] \begin{bmatrix} e(v_{dc})u_1 \\ \dot{e}(v_{dc})u_2 \end{bmatrix}.$$
 (19)

Figure 4 illustrates the external voltage control loop for the DC voltage using sliding mode control (SM-C).

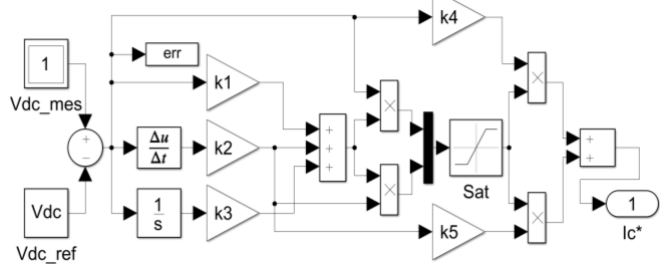


Fig. 4 – The external loop for DC voltage regulation using SM-C.

The adaptive neuro-fuzzy inference system (ANFIS) integrates fuzzy and neural techniques to leverage the benefits of SM-C while mitigating chattering issues inherent in harmonics mitigation using ShAPF. Harmonics from nonlinear loads impact power quality, affecting distribution network stability, especially during changes in irradiation and temperature. ANFIS replaces the discontinuous term in the global control law to reduce chattering, enhancing power

quality and distribution network stability.

3.3 SM CONTROLLER/ANFIS

Recent advancements in artificial intelligence have led to the integration of fuzzy logic (FL) and neural networks (ANN) in hybrid approaches [10,11]. FL controllers offer fast and effective operation without precise mathematical models, while ANNs struggle with limited training data adaptation. A hybrid system, ANFIS, combines FL and ANN to leverage the learning ability of ANN and the reasoning capability of FLC. ANFIS includes input fuzzification, fuzzy operators, modulation, rule compilation, and defuzzification [18, 19]. Its structure resembles the Sugeno Fuzzy model with five layers, comprising input representation, fuzzification, fuzzy rule estimation, and defuzzification, leading to the final output [22–24]. ANFIS performance depends on transfer function coefficients, membership functions, inputs, and rules, this setup is depicted in Fig. 5 [21]:

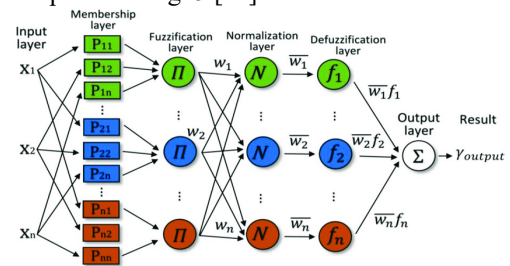


Fig. 5 – ANFIS controller structure.

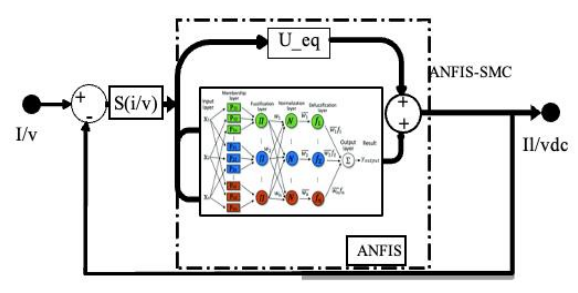


Fig. 6. The configuration of SMC/ANFIS for ShAPF.

The SMC/ANFIS represents an advancement over traditional SM-C by replacing the conventional switching controller term with input from an ANFIS controller. This approach, known as SMC/ANFIS, seeks to enhance the performance of the PV-UPQC while addressing chattering issues associated with conventional SM-C. Its objectives include resolving power quality issues, enhancing distribution network stability, and reducing harmonics from nonlinear loads through the ShAPF. The design of SMC/ANFIS is illustrated in Fig. 6.

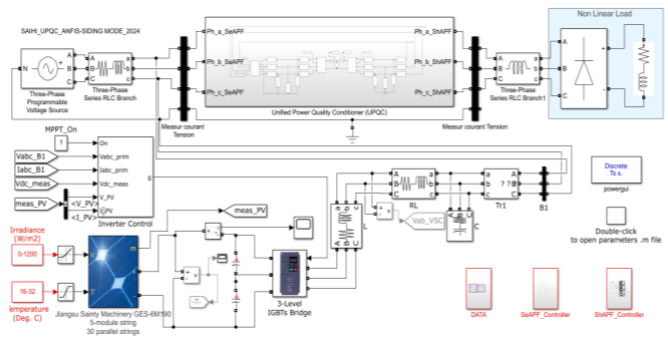


Fig. 7 – PV-UPQC based on SMC/ANFIS.

The control approach implemented using SMC/ANFIS for currents and v_{dc} is outlined as follows:

$$\begin{bmatrix}
v_{fd}^* \\ v_{fq}^* \\ \end{bmatrix} = \begin{bmatrix} u_{fd} \\ u_{fq} \end{bmatrix} = \begin{bmatrix} u_{fd}^{eq} \\ u_{fq}^{eq} \end{bmatrix} + \begin{bmatrix} u_{fd}^{dis_ANIFS} \\ u_{fd}^{dis_ANFIS} \\ u_{dc}^{dis_ANFIS} \end{bmatrix} \\
\begin{bmatrix} u_{v_{dc}} \end{bmatrix} = \begin{bmatrix} k_4 & k_5 \end{bmatrix} \begin{bmatrix} u_{dc}^{dis_ANFIS} (v_{dc}^* - v_{dc}) \\ u_{dc2}^{dis_ANFIS} \frac{d(v_{dc}^* - v_{dc})}{dt} \\ u_{dc2}^{dis_ANFIS} \end{bmatrix}.$$
(19)

Figure 7 presents the detailed PV-UPQC system integrated with the SMC/ANFIS strategy.

4. SITE AND DATA LOCATION

The Adrar region, located in southwest Algeria (as shown in Fig. 8), is renowned for its high solar irradiation levels and elevated temperature averages. The data used in this study were obtained from the URER/MS meteorological station in Adrar, which is affiliated with the Centre for Renewable Energy Development (CDER). Situated at coordinates 27.52° N, 0.18° W and an elevation of 292 meters, this station provides critical meteorological data essential for this research [21,25].

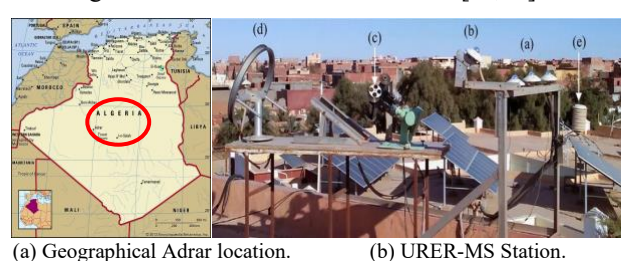


Fig. 8 – Data and site location.

Figure 9 illustrates the recorded temperature and irradiation data in Adrar on June 11, 2023, spanning from 6 am to 8 pm.

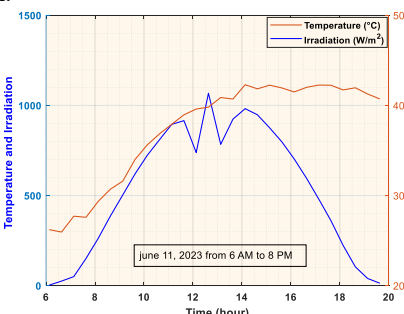


Fig. 9 - Solar conditions (temperature and irradiation) measurements.

5. NUMERICAL SIMULATIONS

In this section, numerical simulations were conducted using the Power Systems Toolbox to evaluate the performance of the PV-UPQC system. Fig. 11 illustrates the system's behavior before and after integrating the ShAPF, enabling a comparison between the PI controller, classical SMC, and the novel SMC/ANFIS controller. Key system parameters are summarized in Table 1, providing valuable information about the simulation setup.

Table 1
System parameter values.

* *		
Parameters	Symbols	Values
Network	E f	$\frac{380}{\sqrt{3}} = 219.39 \text{ V}$ 50 Hz
Load resistor	Rf	0.0080Ω
Load inductance	Lf	0.0059 H
Load capacitor	Cf	0 μF
Filter resistor	RL	0.0080Ω
Filter inductance	LL	0.0029 H
Load capacitor	Cf	5.9422 μF
DC-link voltage	vdc	850 v

5.1 PRE-FILTERING

Figures 10(a) to 10(d) highlight power quality issues observed without the integration of the Shunt Active Power Filter (ShAPF). These include non-sinusoidal currents, dominance of reactive power, poor power factor, and high total harmonic distortion (THD) in the source current. The integration of the ShAPF aims to address these issues and improve power quality.

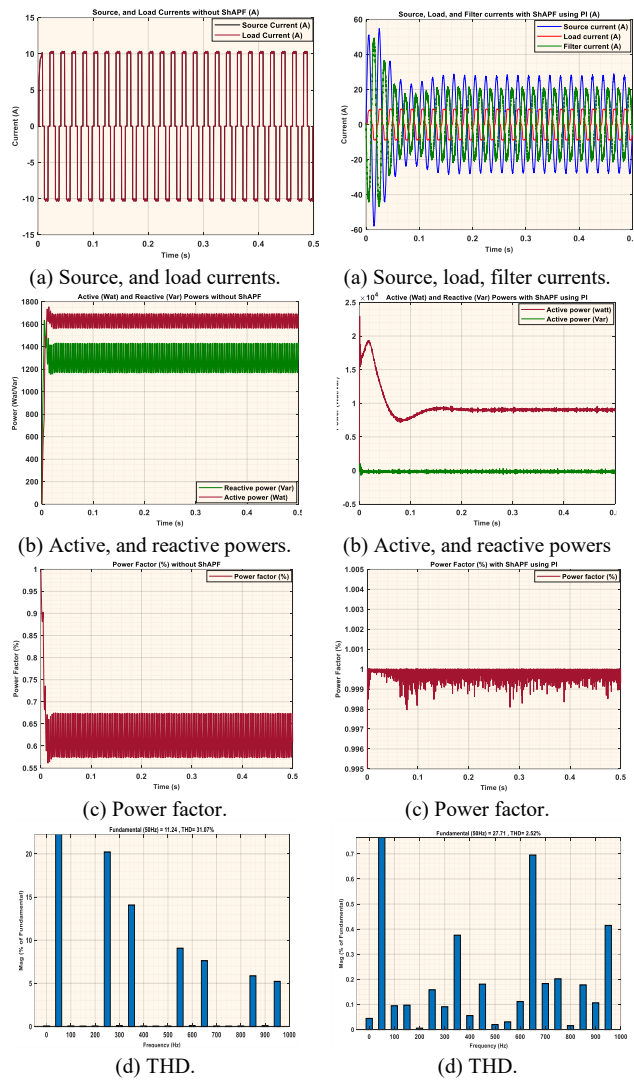


Fig. 10 - Without using ShAPF.

Fig. 11 – With using ShAPF-PI..

5.2 POST-FILTERING

This section presents numerical simulation results evaluating the effectiveness of the proposed SMC/ANFIS strategy in PV-UPQC systems. Simulations compare the performance of PI control, classical SMC, and SMC/ANFIS in regulating reference currents and DC bus voltage, considering nonlinear loads. Figures 11, 12, and 13 illustrate various parameters such as source current, load current, ShAPF current, active/reactive power, power factor, and total harmonic distortion (THD) for each control strategy.

All techniques achieve the primary goal of sinusoidal source current and effectively attenuate harmonics from nonlinear loads, enhancing power factor by reducing reactive power consumption. However, inadequate PI controller regulation and chattering effects in classical SMC may compromise energy quality. The integration of ShAPF, crucial in absorbing nonlinear load harmonics, ensures a sinusoidal source current, further improved with SMC/ANFIS. This

enhancement is consistent across all control strategies.

Moreover, ShAPF significantly reduces reactive power consumption, leading to a power factor close to unity, notably improved with SM/ANFIS. SMC/ANFIS achieves a power factor range of 0.998 to 1, surpassing PI and classical SMC. Additionally, THD of the source current is notably reduced with SMC/ANFIS, meeting IEEE-519 standard specifications. Overall, integrating ShAPF with SMC/ANFIS improves power quality and mitigates harmonic currents, demonstrating significant enhancements in system performance and efficiency in power distribution systems.

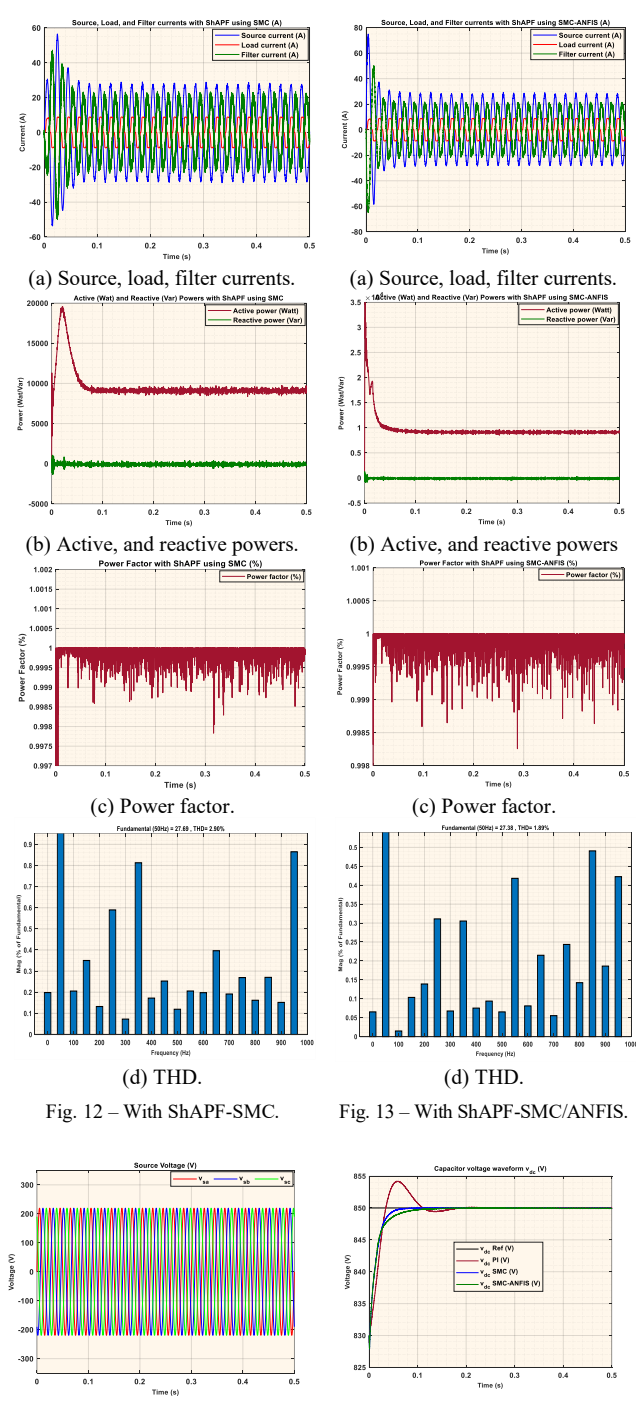


Figure 14 illustrates the source voltages, which exhibit sinusoidal waveforms with a magnitude of $\frac{380}{\sqrt{3}} = 219.39 \text{ V}$. In Fig. 15, the DC-bus voltage is shown reaching the target value of 850 V, starting from an initial value of 830 V, which aligns with the Maximum Power Point Tracking (MPPT) of

Fig.15 – DC-bus voltage.

Fig. 14 – Source voltage.

the solar PV array. While the PI controller exhibits deviations, both the classical SM and SMC/ANFIS controllers maintain precise tracking without deviations. Upon activation of the ShAPF, the DC bus voltage decreases, with the SMC/ANFIS controller demonstrating superior performance in terms of response characteristics, including a shorter response time and reduced overshoot compared to the classical SM technique.

6. CONCLUSION

The application of the sliding mode control-adaptive neurofuzzy inference systems (SMC-ANFIS) method in photovoltaic-unified power quality conditioner (PV-UPQC) systems under real-world conditions, such as those in Adrar, Algeria (accounting for temperature and irradiation), significantly enhances power quality. This method excels in managing harmonic currents and compensating for reactive power by replacing the discontinuous law of the classical sliding mode controller. Outperforming traditional methods like classical sliding mode control (SMC), it reduces chattering effects and improves system stability compared to the classical PI controller.

The inclusion of the shunt active power Filter (ShAPF) further enhances power quality by mitigating harmonics produced by nonlinear loads and improving the power factor. This innovative approach effectively addresses grid integration challenges, positioning it as a promising and robust solution for modern power distribution systems.

CREDIT AUTHORSHIP CONTRIBUTION STATEMENT

Author 1: conceptualization, methodology, software, validation, formal analysis, investigation, writing – original draft, visualization. Author 2: data curation, resources, writing – review & editing, supervision, project administration.

Received on 26 May 2024

REFERENCES

- S. Devassy and B. Singh, Design and performance analysis of threephase solar PV integrated UPQC, IEEE Transactions on Industry Applications, 54, 1, pp. 73–81 (2017).
- R. Thangella, S.R. Yarlagadda, and J. Sanam, Optimal power quality improvement in a hybrid fuzzy-sliding mode MPPT control-based solar PV and BESS with UPQC, International Journal of Dynamics and Control, 11, 4, pp. 1823–1843 (2023).
- A. Amirullah, A. Ananda, O. Penangsang, and A. Soeprijanto, Load active power transfer enhancement using UPQC-PV-BES system with fuzzy logic controller, International Journal of Intelligent Engineering and Systems, 13, 2, pp. 329–349 (2020).
- R. Sekar, M. Arunachalam, and K. Subramanian, Fuzzy-proportional integral derivative controller with interactive decision Tree, Rev. Roum. Sci. Techn. – Électrotechn. et Énerg., 69, 4, pp. 395–400 (2024).
- A. Moghassemi, S. Padmanaban, V.K. Ramachandaramurthy, M. Mitolo, and M. Benbouzid, A novel solar photovoltaic fed TransZSI-DVR for power quality improvement of grid-connected PV systems, IEEE Access, 9, pp. 7263–7279 (2020).
- B. Deffaf, F. Hamoudi, and N. Debdouche, Sliding mode control of a shunt active filter-comparative analysis with conventional PI control, In 19th International Multi-Conference on Systems, Signals & Devices (SSD), pp. 1422–1427 (2022).
- M.T. Benchouia, I. Ghadbane, A. Golea, K. Srairi, and M. Benbouzid, Design and implementation of sliding mode and PI controllers-

- based control for three-phase shunt active power filter, Energy Procedia, **50**, pp. 504–511 (2014).
- J. Morales, L.G. de Vicuna, R. Guzman, M. Castilla, and J. Miret, Modeling and sliding mode control for three-phase active power filters using the vector operation technique, IEEE Transactions on Industrial Electronics, 65, 9, pp. 6828–6838 (2018).
- Y. Chu, J. Fei, and S. Hou, Dynamic global proportional integral derivative sliding mode control using radial basis function neural compensator for three-phase active power filter, Transactions of the Institute of Measurement and Control, 40, 12, pp. 3549–3559 (2018).
- Y. Chu, S. Hou, and J. Fei, Continuous terminal sliding mode control using novel fuzzy neural network for active power filter, Control Engineering Practice, 109, 104735 (2021).
- R. Kumar, Fuzzy particle swarm optimization control algorithm implementation in photovoltaic integrated shunt active power filter for power quality improvement using hardware-in-the-loop, Sustainable Energy Technologies and Assessments, 50, 101820 (2022).
- S.L.K. Bharathi and S. Selvaperumal, MGWO-PI controller for enhanced power flow compensation using unified power quality conditioner in wind turbine squirrel cage induction generator, Microprocessors and Microsystems, 76, 103080 (2020).
- A. Chebabhi, M.K. Fellah, A. Kessal, and M.F. Benkhoris, Comparative study of reference currents and DC bus voltage control for Three-Phase Four-Wire Four-Leg SAPF to compensate harmonics and reactive power with 3D SVM, ISA transactions, 57, pp. 360–372 (2015).
- K. Sozanski and P. Szczesniak, Advanced control algorithm for threephase shunt active power filter using sliding DFT, Energies, 16, 3, 1453 (2023).
- E. Samavati and H.R. Mohammadi, Active harmonic compensation and stability improvement in high-power grid-connected inverters using unified power quality conditioner, International Journal of Industrial Electronics Control and Optimization, 6, 3, pp. 193

 –204 (2023).
- S. Chennai, Novel shunt active power filter based on nine-Level NPC inverter using MC-LSPWM modulation strategy, Rev. Roum. Sci. Techn. – Électrotechn. et Énerg., 69, 1, pp. 21–26 (2024).
- H. Usman and N. Magaji, Simulation of shunt active power filter based fuzzy logic controller for minimization of total harmonic distortion, Int. J. of Applied and Advanced Engineering Research, 2, 1 (2023).
- L. Saihi, F. Ferroudji, K. Roummani, K. Koussa, Y. Bakou, and B. Berbaoui, Improved harmonic mitigation with a SAP filter connected to a renewable energy source using a novel ANN algorithm, Second International Conference on Energy Transition and Security (ICETS), pp. 1–6 (2023).
- L. Saihi and B. Berbaoui, Mitigation of low voltage electrical network pollution using a two-level PAPF controlled by the ANN-PQ algorithm, International Conference on Electrical Engineering and Advanced Technology (ICEEAT), 1, pp. 1–5 (2023).
- R. Rouabhi, A. Herizi, S. Djeriou, and A. Zemmit, Hybrid type-1 and 2 fuzzy sliding mode control of the induction motor, Rev. Roum. Sci. Techn. Électrotechn. et Énerg., 69, 2, pp. 147–152 (2024).
- L. Saihi and B. Berbaoui, Sliding mode of second-order control based on super-twisting ANFIS algorithm of doubly fed induction generator in wind turbine systems with real variable speeds, Iranian Journal of Science and Technology, Transactions of Electrical Engineering, 47, 2, pp. 473–490 (2023).
- S. Latreche, A. Bouafassa, B. Babes, and O. Aissa, Efficient DSP-based real-time implementation of ANFIS regulator for single-phase power factor corrector, Rev. Roum. Sci. Techn. – Électrotechn. et Énerg., 69, 2, pp. 141–146 (2024).
- R. Bhavani, N.R. Prabha, and M.A. Jawahar, An ultra-capacitor integrated dynamic voltage restorer for power quality enhancement in a three-phase distribution system using an adaptive neuro-fuzzy interference system controller, Rev. Roum. Sci. Techn. Électrotechn. et Énerg., 67, 4, pp. 383–388 (2022).
- S. Lakhdar, F. Ferroudji, K. Roummani, and K. Koussa, Enhanced sensor-less control of DFIG-based generators using hybrid MRAS-ANN observer and PSO parameter optimization, In 14th International Renewable Energy Congress (IREC), pp. 1–6 (2023).
- I. Oulimar, K. Bouchouicha, N. Bailek, and M. Bellaoui, Statistical study
 of global solar radiation in the Algerian desert: a case study of Adrar
 town, Theoretical and Applied Climatology, pp. 1–12 (2024).